Journal of Solid State Chemistry **163,** 540–545 (2002)
doi:10.1006/jssc.2001.9366, available online at http://www.idealibrary.com on IDEAL®

Modulated Structure of the Composite Crystal $Ca_{0.83}CuO_2$

Y. Miyazaki,*,†,[1] M. Onoda,‡ P. P. Edwards,† S. Shamoto,* and T. Kajitani*

*Department of Applied Physics, Graduate School of Engineering, Tohoku University, Aramaki Aoba, Aoba-ku, Sendai 980-8579, Japan; †School of Chemistry, University of Birmingham, Edgbaston, Birmingham B15 2TT, United Kingdom; and ‡Advanced Materials Laboratory, National Institute for Materials Science, Namiki, Tsukuba, Ibaraki 305-0044, Japan

Received May 30, 2001; in revised form August 13, 2001; accepted August 17, 2001

We have determined the crystal structure of the quasi one-dimensional cuprate $Ca_{0.83}CuO_2$, known as $Ca_4Cu_5O_{10}$, etc., by a superspace group approach. The compound consists of two interpenetrating subsystems of CuO_2 chains and Ca atoms. Structural parameters were refined with a superspace group of $F2/m(1+\alpha\ 0\ \gamma)0s$ using powder X-ray and neutron diffraction data. Lattice parameters were refined to be $a_1 = 2.8043(2)$ Å, $b = 6.3179(2)$ Å, $c_1 = 10.5744(5)$ Å, and $\beta_1 = 90.10(1)^\circ$ for the $[CuO_2]$ subsystem and $a_2 = 3.3652(2)$ Å, $b = 6.3179(2)$ Å, $c_2 = 10.5893(5)$ Å, and $\beta_2 = 93.04(1)^\circ$ for the [Ca] subsystem. Remarkable displacive modulation of the O and Ca atom sites is observed parallel to the *b*-axis and the *c*-axis, respectively. On the other hand, the Cu atom sites deviate mainly in the *a* direction to yield a periodic fluctuation between the nearest Cu–Cu distances. The Ca atoms suitably sit in the center of the modulated O_6 octahedra. © 2002 Elsevier Science (USA)

Key Words: **low-dimensional compound; composite crystal; superspace group; cuprate; Rietveld refinement.**

INTRODUCTION

Quasi one-dimensional (1D) cuprate $Ca_{1-x}CuO_2$ ($x \sim 0.15$) has recently attracted much interest owing to its unique magnetism (1–5) and crystal structure (3, 6–11). Since the compound has an in-built Ca deficiency, the formal Cu valence (Cu^{n+}) becomes ~ 2.3, where approximately one-third of the Cu sites are hole–doped nonmagnetic ($S = 0$) state. Extensive studies have been performed to investigate the present compound as a diluted $S = \frac{1}{2}$ magnetic system, revealing that the magnetic behavior can be well described as a mixture of Curie–Weiss, spin dimer, and/or alternating Heisenberg chain components (1, 4, 5, 12). Most of the doped holes are believed to be localized, leading to the dilution of long-range spin correlations. The crystal structure of the compound on the other hand, has not yet been fully determined. Several chemical formulas, $Ca_{0.828}CuO_2$ (13), $Ca_{0.83}CuO_2$ (2), $Ca_{0.85}CuO_2$ (1, 7–10), $Ca_4Cu_5O_{10}$ (6, 14, 15), $Ca_{1-x}CuO_2$ (4, 5, 11), etc. have been proposed to express this compound but the precise composition is still controversial. Earlier structure work made by Siegrist *et al.* (6) and Babu and Greaves (7) demonstrated that the basic structure is closely related to that of $NaCuO_2$ (16). The stoichiometric compound belongs to a monoclinic system, $C2/m$, with lattice parameters of $a = 6.3512(2)$ Å, $b = 2.7474(1)$ Å, $c = 6.1027(2)$ Å, and $\beta = 120.767(2)^\circ$. The structure consists of 1D CuO_2 chains with sharing opposite edges of CuO_4 squares and Na atoms locating between the chains to form the NaO_6 octahedra. The Ca-deficient analogue, in contrast, shows superlattice reflections in the diffraction patterns due to a periodic difference between the Ca atoms and the CuO_2 chains. An atomic displacive modulation usually occurs in such a "composite crystal" through mutual interactions between the subsystems. One can obtain an approximate structure of a composite crystal through conventional structure refinement methods by assuming statistical distribution of the atoms (6, 7). Taking a larger unit cell with nearly commensurate composition often gives more adequate solution of the structure (17). However, such a structure analysis usually yields a large number of refinable parameters and it often causes obscure understanding of the structure. In contrast, introduction of a higher dimensional superspace group into the structure analysis allows a simple description of the composite crystal. Moreover, this approach makes a uniform treatment of the compound system, which changes its stoichiometry incommensurately, as observed in the present solid solution system, $(Ca_{1-y}Y_y)_{1-x}CuO_2$ (11). In this study, we have refined the crystal structure of the title compound by means of a four-dimensional superspace group approach. Rietveld refinement, using a set of powder X-ray and neutron diffraction data, has precisely revealed the remarkable modulated arrangement of the "CuO_2 ribbons" along the *a* axis.

EXPERIMENTAL

Polycrystalline samples were prepared by the standard solid-state reaction method. Appropriate amounts of

[1]To whom correspondence should be addressed. E-mail: miya@crystal.apph.tohoku.ac.jp. Fax: +81-22-263-9836.

0022-4596/02 $35.00

$CaCO_3$ (99.9%) and CuO (99.99%) powders were mixed with an agate mortar and pressed into pellets. The pellets were heated at 830°C for 20 h under flowing oxygen gas. Then, the samples were furnace cooled to room temperature, ground, and pelletized again. Higher sintering temperature resulted in the formation of Ca_2CuO_3 but this phase gradually disappeared when further sintered at 830°C. Total sintering time of 360 h is necessary to obtain well-crystallized single-phase samples under 1 atm of oxygen gas.

X-ray diffraction (XRD) data were collected with Cu$K\alpha$ radiation at room temperature in the 2θ angular range of 10–100° with a 0.040° step using a Rigaku RAD-C diffractometer equipped with a curved graphite monochromator. Neutron powder diffraction (ND) data were collected at room temperature by the use of the HERMES diffractometer of the Institute for Materials Research (IMR), Tohoku University, installed at the JRR-3M reactor in the Japan Atomic Energy Research Institute (JAERI) (18). The incident neutron beam was monochromatized to $\lambda = 1.8196$ Å. The XRD and ND data were analyzed simultaneously using a Rietveld refinement program, PREMOS 91 (19), designed for modulated structure analyses. Crystal structures and interatomic distance plots were drawn with PRJMS and MODPLT routines; both are included in the PREMOS 91 package.

RESULTS AND DISCUSSION

Structure Refinement

The structure model was constructed on the basis of the report by Miyazaki *et al.* (11) in which a face centered monoclinic unit cell was adopted. We assigned the CuO_2 chains to subsystem 1 and the Ca atoms to subsystem 2. All the XRD and ND reflections were indexed assuming two monoclinic unit cells with a common b axis ($b \sim 6.32$ Å) and different a and c axes: $a_1 \sim 2.80$ Å for subsystem 1 and $a_2 \sim 3.36$ Å for subsystem 2. The relationship between the c-axis lengths of both subsystems is $c_1 \sin\beta_1 = c_2 \sin\beta_2$. Four integers, $HKLM$, are required to fully index those reflections, including satellite peaks that originated from the interaction between the subsystems. The reciprocal base vectors of the Ca subsystem, ($\boldsymbol{a}_2^*$, $\boldsymbol{b}_2^*$, $\boldsymbol{c}_2^*$), can be expressed using those of the CuO_2 subsystem, ($\boldsymbol{a}_1^*$, $\boldsymbol{b}_1^*$, $\boldsymbol{c}_1^*$), as $\boldsymbol{a}_2^* = \alpha\boldsymbol{a}_1^* + \gamma\boldsymbol{c}_1^*$, $\boldsymbol{b}_2^* = \boldsymbol{b}_1^*$, $\boldsymbol{c}_2^* = \boldsymbol{c}_1^*$. The observed systematic absences of the reflections are as follows: $H + K + M = 2n$, $H + L + M = 2n$, and $K + L = 2n$ for $HKLM$; $M = 2n$ for $H0LM$. From these conditions, the allowed symmetry for both subsystems are $F2$, Fm, and $F2/m$ and we chose the highest symmetry of $F2/m$ for both subsystems. The generator set of the superspace group can be expressed as $x_1 + \frac{1}{2}$, $x_2 + \frac{1}{2}$, x_3, $x_4 + \frac{1}{2}$; $x_1 + \frac{1}{2}$, x_2, $x_3 + \frac{1}{2}$, $x_4 + \frac{1}{2}$; $-x_1$, x_2, $-x_3$, $-x_4 + \frac{1}{2}$; $-x_1$, $-x_2$, $-x_3$, $-x_4$. Then, we adopted a suitable superspace group of $F2/m(1 + \alpha\ 0\ \gamma)0s$, being equivalent to $B2/m(\alpha\,\beta\,0)0s$ (No. 12.2) in Table 9.8.3.5 in Ref. (20). Atomic scattering factors and bound coherent neutron scattering lengths were respectively taken from Tables 6.1.1.4 and 4.4.4.1 in Ref. (20). The refinement was made using the total number of reflections of 425 for ND data and of 351 for XRD data, including satellite peaks. Table 1 summarizes the initial fractional coordinates and isotropic atomic displacement parameters, B, of the atoms of the fundamental structure. After several refinement cycles, the displacive modulation of the atomic positions was introduced, considering up to the second order of cosine and sine components of the Fourier terms, i.e., $A_i (i = 0, 1, 2)$ and $B_i (i = 1, 2)$. Table 2 summarizes refined Fourier amplitudes for the fractional coordinates and B factors. The refined modulation vector components along the a^* and c^* axes, α and γ, are also shown in the table. The numbers in parentheses represent estimated standard deviations of the last significant digits. The averaged structure can be

TABLE 1
Initial Fractional Coordinates and Isotropic Atomic Displacement Parameters, B, for the Fundamental Structure of $Ca_{0.83}CuO_2$

Subsystem 1: [CuO_2]	$x(=x_1)$	$y(=x_2)$	$z(=x_3)$	B(Å^2)
Cu	0.0	0.0	0.0	1.0
O	0.002	0.0	0.380	1.0
Subsystem 2: [Ca]	$x(=x_4)$	$y(=x_2)$	$z(=x_3)$	B(Å^2)
Ca	0.0	$\frac{1}{4}$	$\frac{1}{4}$	1.0

TABLE 2
Refined Fourier Amplitudes and Modulation Vector Components α and γ of $Ca_{0.83}CuO_2$

Atom		A_0	A_1	B_1	A_2	B_2
		Subsystem 1: [CuO_2]				
Cu	$x(=x_1)$	0	0	0	0	−0.009(4)
	$y(=x_2)$	0	0	−0.012(1)	0	0
	$z(=x_3)$	0	0	0	0	−0.001(1)
	B	−0.31(9)	0	0	0.9(3)	0
O	$x(=x_1)$	−0.011(3)	0	0	0.007(5)	−0.035(4)
	$y(=x_2)$	0	0.065(1)	0.005(2)	0	0
	$z(=x_3)$	−0.0053(4)	0	0	−0.003(1)	−0.012(1)
	B	−0.23(11)	0	0	0.3(2)	1.4(2)
		Subsystem 2: [Ca]				
Ca	$x(=x_4)$	0	0	0	0	0.013(8)
	$y(=x_2)$	0	0	−0.003(3)	0	0
	$z(=x_3)$	0	0	0	0	0.011(2)
	B	−0.36(18)	0	0	−1.4(6)	0

Modulation vector components: $\alpha = 0.8333(2)$, $\gamma = 0.1650(9)$

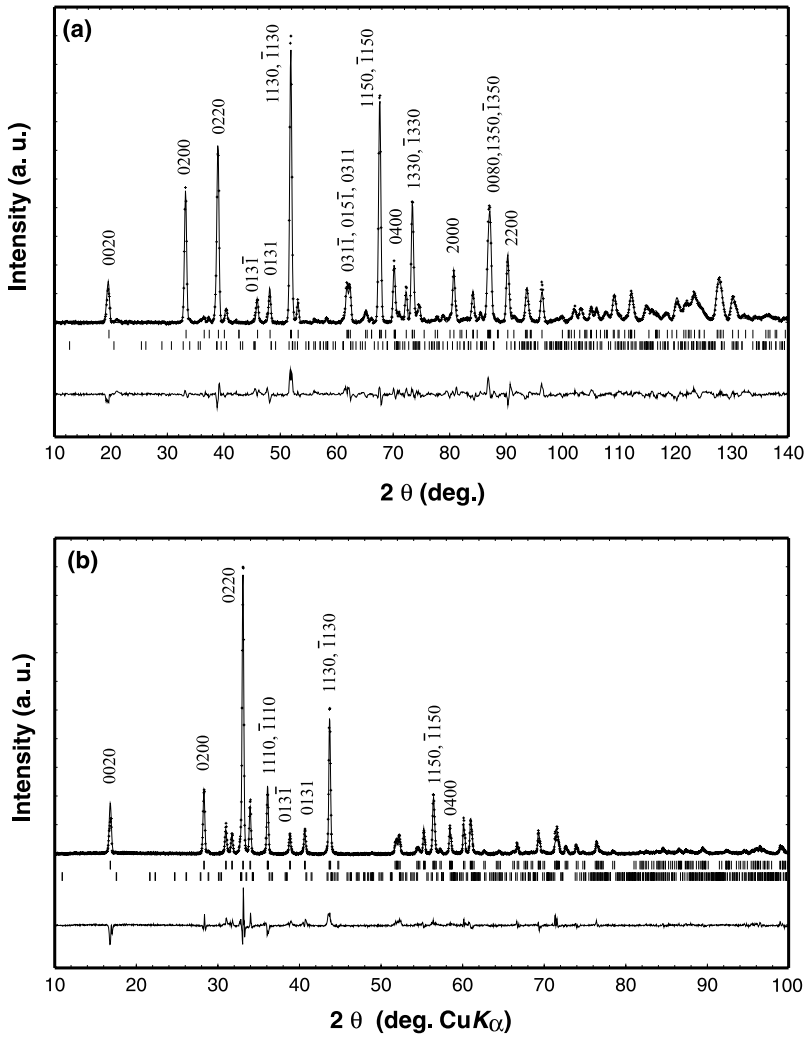

FIG. 1. Observed, calculated, and difference patterns of the (a) neutron and (b) X-ray diffraction data for $Ca_{0.83}CuO_2$. Short vertical lines below the patterns indicate the peak positions of main (upper) and satellite (lower) reflections for the two subsystems. The difference between the observed and calculated intensities are shown below the vertical lines.

obtained by adding A_0 terms to the corresponding parameters of the fundamental structure shown in Table 1. Due to the superspace group symmetry, the number of refinable parameters of the Fourier terms is limited as shown in Table 2. The total number of the refinable parameters was 58 including 21 positional parameters, 30 profile parameters (15 for ND and 15 for XRD), and 7 lattice parameters. Each set of the profile parameters contains 1 scale factor, 6 background, 7 peak-shape, and 1 zero-point shift parameters. The modulation vector components, α and γ, were refined to be 0.8333(2) and 0.1650(9), respectively.

Figure 1 shows observed, calculated, and difference profiles for the ND (a) and XRD (b) data. Short vertical lines below the patterns indicate the peak positions of main (upper) and satellite (lower) reflections for the two subsystems. The final R_{wp} factors were 9.8% for the ND data and 6.2% for the XRD data. Lattice parameters were refined to be $a_1 = 2.8043(2)$ Å, $b = 6.3179(2)$ Å, $c_1 = 10.5744(5)$ Å, and $\beta_1 = 90.10(1)^\circ$ for subsystem 1 and $a_2 = 3.3652(2)$ Å, $b = 6.3179(2)$ Å, $c_2 = 10.5893(5)$ Å, and $\beta_2 = 93.04(1)^\circ$ for subsystem 2. The resulting a_1/a_2 $(= \alpha)$ ratio of 0.8333(2) corresponds to the stoichiometry of the sample, $Ca_{0.8333}CuO_2$. It should be noted here that the oxygen stoichiometry of the compound depends on the preparation routes. For example, a small amount of oxygen deficiency, $\delta \sim -0.03$ in $Ca_{0.83}CuO_{2+\delta}$, has been reported for the sample prepared under flowing oxygen gas (5). On the other hand, the samples prepared under high pressure of 3–6 GPa show a very small amount of excess oxygen as $\delta \sim 0.01$ (5). We attempted to refine the oxygen content of our sample but no deviation in the occupation factor was observed and thus we fixed the parameter at 1.0 in the final refinement cycles.

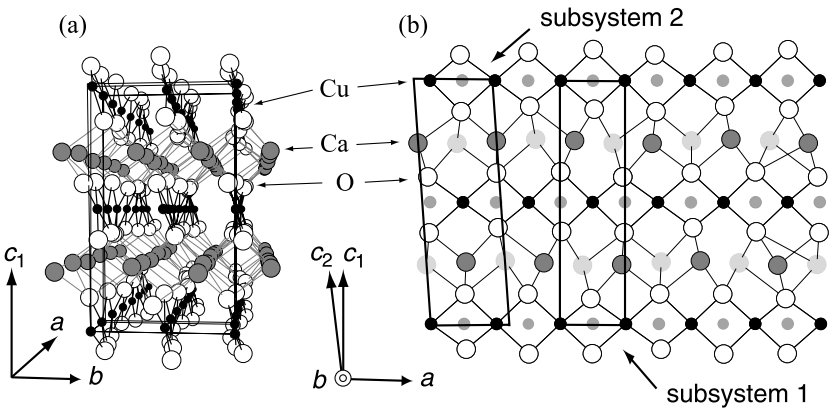

FIG. 2. The refined modulated crystal structure of $Ca_{0.83}CuO_2$ viewed (a) in perspective from $[\bar{1}00]$ and (b) from [010].

Structure Details

Figure 2a shows the refined modulated structure viewed in perspective from $[\bar{1}00]$. One might recognize markedly waved rows of the O atoms forming "CuO_2 ribbons" along the *a* axis. In contrast, the Ca atoms appear to fluctuate mainly in the *c* axis. These displacive modulations originated from the interactions between the two subsystems, namely, the CuO_2 chains and the Ca atoms, which have different periods along the *a* axis. Both unit cells are illustrated as thick lines in Fig. 2b viewed from the *b* axis. The Cu atoms are represented as small closed ($y \sim 1.0$) and small shaded ($y \sim \frac{1}{2}$) circles. Large thicker and thinner circles correspond to the Ca atoms located at $y \sim \frac{3}{4}$ and $y \sim \frac{1}{4}$, respectively. For clarity, only the O atoms at the coordinate of $y \sim 1.0$ are shown. The modulation of the atom sites can be further understood from Figs. 3a and 3b; both are viewed from the *c* axis but the included region is different: $z = 0.7$–1.2 for (a) and $z = 0.6$–1.1 for (b). As shown in Figs. 3a and 3b, every Ca atom is coordinated to six O atoms, with three lower and three upper ones along the *c* axis, forming a CaO_6 octahedron. The O atoms appear to shift cooperatively so as to accomodate the Ca atoms in the center of the O_6 cages. Each CaO_6 octahedron shares its edge with an adjacent one but the octahedron is disconnected at every third CaO_6 units along the *a* axis.

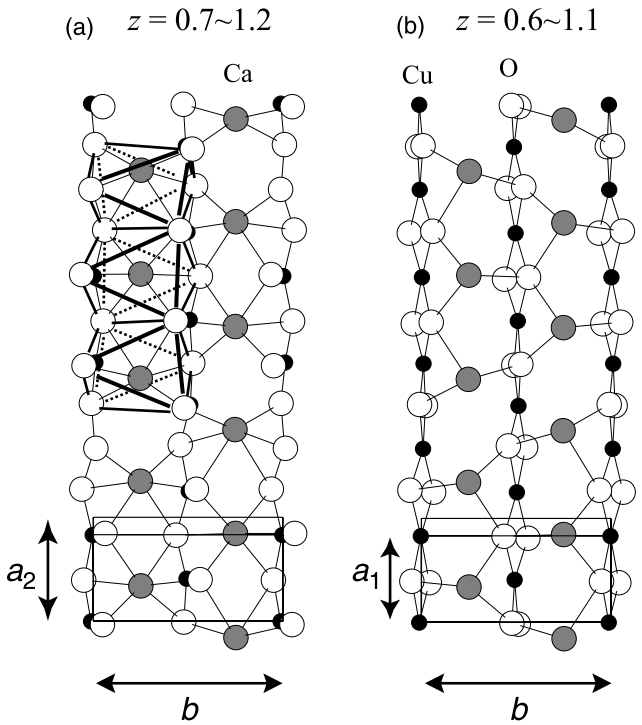

FIG. 3. Modulated structure of $Ca_{0.83}CuO_2$ projected along [001] for a range of (a) $z = 0.7$–1.2 and (b) $z = 0.6$–1.1.

Next, interatomic distances were calculated from the refined parameters. Figure 4 shows the Ca–O distance (d_{Ca-O}) plotted against $t'(= -\alpha x_1 - \gamma x_3 + x_4 = -0.8333x_1 - 0.1650x_3 + x_4)$, a complementary (four-dimensional) coordinate in the superspace (19). Any section with different t' values corresponds to a different phase of the modulation wave in the modulated structure. The letters *a*, *b*, ..., and *n* represent symmetry codes for O atoms as denoted in the caption of Fig. 4. Two O atoms approach a Ca atom to reach minimum lengths of (d_{Ca-O}) ~ 2.15 Å and then depart away and the next two O atoms approach as t' increases. In the vicinity of the points where six lines come across, the Ca atoms have almost identical bond lengths of *ca.* 2.35 Å with O atoms. This bond length is comparable to the value reported in another calcium copper oxide, Ca_2CuO_3 of $d_{Ca-O} = 2.33$–2.50 Å (21). The stoichiometric compound $NaCuO_2$ also consists of the CuO_2 chains and the counter Na atoms but it shows no modulation because the periods of the CuO_2 chains and the Na atoms are equal. The compound has only one kind of NaO_6 octahedron in which the Na–O distances are $2 \times 2.411(1)$ Å (apical) and

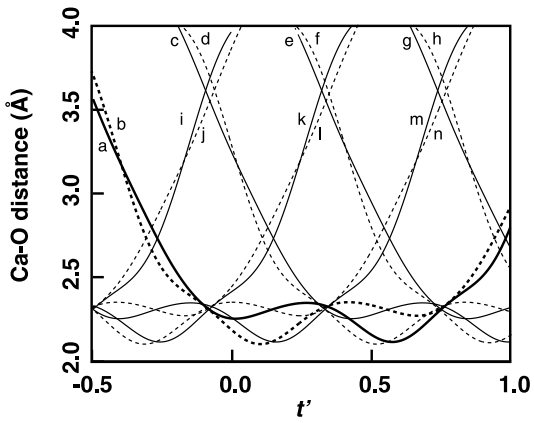

FIG. 4. Ca–O distances, d_{Ca-O}, plotted against a complementary coordinate, $t'(=-\alpha x_1-\gamma x_3+x_4=-0.8333x_1-0.1650x_3+x_4)$ in the superspace. The letters *a*, *b*, … and *n*, represent symmetry codes for O atoms as follows. (a) $-x-\frac{1}{2}, y+\frac{1}{2}, -z+1$; (b) $x-\frac{1}{2}, y, z-\frac{1}{2}$; (c) $-x-1, y, -z+1$; (d) $x-1, y+\frac{1}{2}, z-\frac{1}{2}$; (e) $-x-\frac{3}{2}, y+\frac{1}{2}, -z+1$; (f) $x-\frac{3}{2}, y, z-\frac{1}{2}$; (g) $-x-2, y, -z+1$; (h) $x-2, y+\frac{1}{2}, z-\frac{1}{2}$; (i) $-x+1, y, -z+1$; (j) $x+1, y+\frac{1}{2}, z-\frac{1}{2}$; (k) $-x+\frac{1}{2}, y+\frac{1}{2}, -z+1$; (l) $x+\frac{1}{2}, y, z-\frac{1}{2}$; (m) $-x, y, -z+1$; (n) $x, y+\frac{1}{2}, z-\frac{1}{2}$.

$4\times2.360(3)$ Å (equatorial). All the Cu ions in $NaCuO_2$ are in a trivalent state, with a much shorter Cu–O distance of $4\times1.839(1)$ Å than that obtained by our refinement shown in the next section.

Figure 5 shows the Cu–O distance (d_{Cu-O}) in the CuO_2 chain (a) and the Cu–Cu distances (d_{Cu-Cu}) of the nearest and the next nearest sites (b), plotted as a function of t'. The next nearest one corresponds to the interchain Cu–Cu length between the two neighboring CuO_2 chains along the *b* axis. Because the Cu and O atoms belong to the same subsystem (i.e., subsystem 1), both d_{Cu-O} and d_{Cu-Cu} are periodically altered in the interval of $0\le t'\le1$. Each Cu atom is coordinated to four O atoms with the average distances of 2×1.95 Å (lines (i) and (ii)) and 2×2.00 Å (lines (iii) and (iv)). The d_{Cu-O} values of the latter two O atoms largely vary from 1.85 to 2.15 Å, while those of the former are nearly constant at around 1.95 Å. Surprisingly, as shown in Fig. 5b, the nearest Cu–Cu distance (solid line) significantly oscillates from 2.78 to 2.88 Å with the average distance of 2.83 Å, whereas the next nearest d_{Cu-Cu} (dotted line) has a fairly constant value of 3.41 Å. Such a fluctuation of the nearest Cu–Cu distance has not been observed in the Y-doped counterpart, $(Ca_{0.565}Y_{0.435})_{0.82}CuO_2$ (22), where all the Cu atoms are in an equivalent magnetic state of $S=\frac{1}{2}$, expected from $Cu^{n+}=2.00$. The present compound, on the other hand, is known as a heavily hole-doped quasi 1D $S=\frac{1}{2}$ magnetic system, where approximately one-third of the Cu sites form Zhang–Rice ($S=0$) singlets (23). Since the compound is a bad conductor ($\sim10^5\,\Omega$-cm), most of the hole carriers are localized on particular Cu sites. Consequently, an almost ordered arrangement of the $S=\frac{1}{2}$ (consider up and down spins as "↑" and "↓") and $S=0$ (◦) Cu ions, such as the localization of Zhang–Rice singlets at every third Cu sites (↑↓◦↑↓◦ …), would occur to minimize the repulsion between the singlets. The origin of the oscillation in the nearest Cu–Cu distance can be ascribed to the quasi-ordered distribution of magnetically unequivalent Cu ions in the structure.

In this kind of composite crystals, a strong Coulomb effect on the CuO_2 chain would lead to a localization of holes at room temperature. In the present 1D CuO_2 chain, there has been the modulation of Cu–O distances with maximum amplitudes of about 0.3 Å, which can be expected in the Cu_2O_3 ladder between 1D and 2D. In the structural study of the ladder compound $Sr_{13.44}Bi_{0.56}Cu_{24+y}O_{41+z}$, almost no modulation in Cu–O distances of the ladder has been observed (24), while the Cu–O distances modulate significantly with maximum amplitudes of about 0.1 Å along the leg direction in $Ca_{13.6}Sr_{0.4}Cu_{23.983}O_{40.965}$ (24), indicating hole localization in the ladder. The latter result is consistent with the temperature dependence of the resistivity, indicative of charge density wave. With increasing dimensionality, there might be less nesting condition of the Fermi surface. These results, however, suggest that even in a 2D CuO_2 plane, hole segregation could be produced by local lattice distortion at phase boundary, e.g., twin boundary (25). Furthermore, a recent EXAFS study reveals that the superconducting transition temperature in La214 cuprate can be enhanced with the existence of a finite local lattice strain (26). The present amplitude of static Cu–O modulation would give us valuable information on the valence modulation in Cu–O networks.

Finally, our refinement should be compared with that recently reported by Galez *et al.* (17), who analyzed the same compound by a conventional Rietveld method. They assumed a large unit cell of 6-fold length of our a_1 axis, based on the electron diffraction experiment, and presented undulation of the O atoms in the CuO_2 chains. It is acceptable because their sample could have a $6a_1$ commensurate period along the *a* axis. They claimed that parts of the Ca and the O atoms are deficient and concluded the stoichiometry of the compound as $Ca_{4.78}Cu_6O_{11.60}$. However, as we have demonstrated, the compound must be treated as a composite crystal, with two subsystems of CuO_2 chains and Ca atoms, in which every atom occupies only one crystallographical site in the fundamental structure. Contrary to their report, no noticeable deficiency for each atom is observed in our refinement. The compound appears to have a flexibility to accomodate different valence cations in the modulated O_6 cages. Some lanthanides, alkali-earth, and alkali atoms, *M*, have been found to substitute for the Ca site (3, 4, 11, 14–16) to form a solid solution of $(Ca_{1-y}M_y)_{a_1/a_2}CuO_2$. The a_1/a_2 ratio ($=\alpha$), which yields a stoichiometry of the solid solution of the sample, incommensurately varies from *ca.* 0.73 to 1.0. The resulting Cu^{n+} value covers from *ca.* 2.0 to

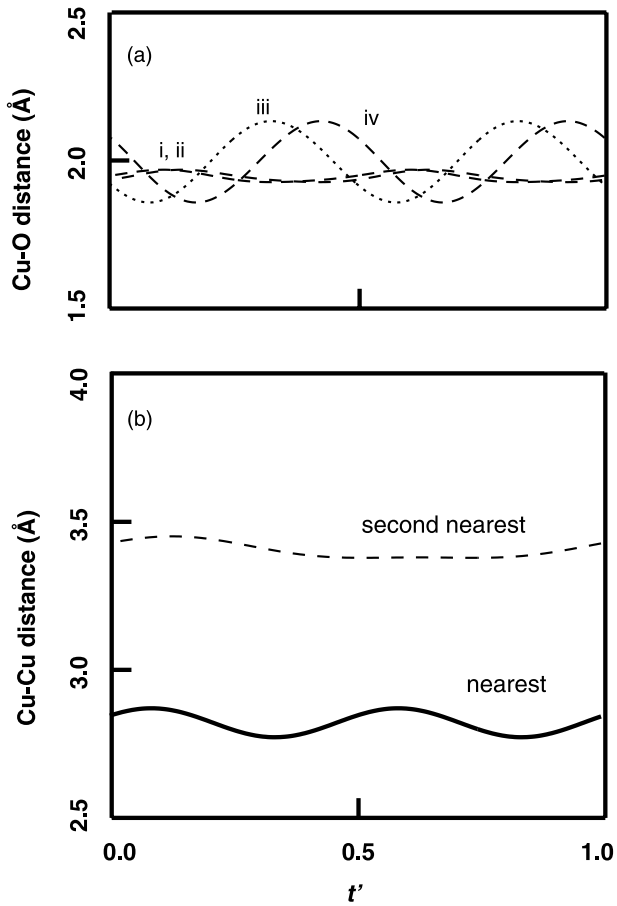

FIG. 5. (a) Cu–O distances, d_{Cu-O}, and (b) the nearest and the next nearest Cu–Cu distances, d_{Cu-Cu}, plotted against a complementary coordinate, t', in the superspace. The letters represent symmetry codes for O atoms as follows. (i) $x, y+\frac{1}{2}, z$; (ii) $x+1, y+\frac{1}{2}, z$; (iii) $-x+1, y+\frac{1}{2}, -z+\frac{1}{2}$; (iv) $-x, y+\frac{1}{2}, -z+\frac{1}{2}$.

3.0, depending on the size and valence of M. Investigation of the magnetic properties of such a solid solution will be intriguing to further understand the diluted quasi 1D magnetic system.

SUMMARY

The modulated structure of $Ca_{0.83}CuO_2$ is successfully determined from X-ray and neutron diffraction data assuming a superspace group of $F2/m(1+\alpha\ 0\ \gamma)0s$, which has the highest possible symmetry. Periodic difference between the CuO_2 and Ca subsystems causes remarkable displacement on each atom. The observed sinusoidal modulation in the nearest Cu–Cu distance may have a connection with a kind of charge-ordered state known as "stripe patterns" in the real space.

ACKNOWLEDGMENT

This work was supported, in part, by the JSPS (Japan Society for the Promotion of Science) Post Doctoral Fellowships for Research Abroad to Y.M.

REFERENCES

1. J. Dolinsek, D. Arcon, P. Cevc, O. Milat, M. Miljak, and I. Aviani, *Phys. Rev. B* **57,** 7798 (1998).
2. G. I. Meijar, C. Rossel, E. M. Kopnin, M. Willemin, J. Karpinski, H. Schwer, K. Conder, and P. Wachter, *Europhys. Lett.* **42,** 339 (1998).
3. A. Hayashi, B. Batlogg, and R. J. Cava, *Phys. Rev. B* **58,** 2678 (1998).
4. Y. Miyazaki, N. C. Hyatt, M. Slaski, I. Gameson, and P. P. Edwards, *Chem. Eur. J.* **5,** 2265 (1999).
5. Z. Hiroi, M. Okumura, T. Yamada, and M. Takano, *J. Phys. Soc. Jpn.* **69,** 1824 (2000).
6. T. Siegrist, R. S. Roth, C. J. Rawn, and J. J. Ritter, *Chem. Mater.* **2,** 192 (1990).
7. T. G. N. Babu and C. Greaves, *Mater. Res. Bull.* **26,** 499 (1991).
8. O. Milat, G. Tendeloo, S. Amelinckx, T. G. N. Babu, and C. Greaves, *J. Solid State Chem.* **97,** 405 (1992).
9. O. Milat, G. Tendeloo, S. Amelinckx, T. G. N. Babu, and C. Greaves, *Solid State Commun.* **79,** 1059 (1991).
10. O. Milat, G. Tendeloo, S. Amelinckx, T. G. N. Babu, and C. Greaves, *J. Solid State Chem.* **101,** 92 (1992).
11. Y. Miyazaki, I. Gameson, and P. P. Edwards, *J. Solid State Chem.* **145,** 511 (1999).
12. Y. Miyazaki, N. C. Hyatt, P. A. Anderson, and P. P. Edwards, *in* "Proc. 12th Int. Symp. Superconductivity (ISS 99), Morioka, 1999" (T. Yamashita and K. Tanabe, Eds.), p. 149. Springer-Verlag, Berlin/New York, 2000.
13. R. S. Roth, N. M. Hwang, C. J. Rawn, B. P. Burton, and J. J. Ritter, *J. Am. Ceram. Soc.* **74,** 2148 (1991).
14. P. K. Davies, E. Caignol, and T. King, *J. Am. Ceram. Soc.* **74,** 569 (1991).
15. P. K. Davies, *J. Solid State Chem.* **95,** 365 (1991).
16. N. E. Brese, M. O'Keeffe, R. B. von Dreele, and V. G. Young, Jr., *J. Solid State Chem.* **83,** 1 (1989).
17. P. Galez, M. L. Tafin, T. Hopfinger, C. Opagiste, and C. Bertrand, *J. Solid State Chem.* **151,** 170 (2000).
18. K. Ohoyama, T. Kanouchi, K. Nemoto, M. Ohashi, T. Kajitani, and Y. Yamaguchi, *Jpn. J Appl. Phys.* **37,** 3319 (1998).
19. A. Yamamoto, *Acta Crystallogr. A* **49,** 831 (1993).
20. "International Tables for Crystallography" (A. J. C. Wilson and E. Prince, Eds.), Vol. C. Kluwer Academic, Dordrecht/Norwell, MA, 1999.
21. C. L. Teske and H. Muller-Buschbaum, *Z. Anorg. Allg. Chem.* **379,** 234 (1970).
22. Y. Miyazaki, M. Onoda, A. Yamamoto, P. P. Edwards, and T. Kajitani, *J. Phys. Soc. Jpn.* **70**(Suppl. A), 238 (2001).
23. F. C. Zhang and T. M. Rice, *Phys. Rev. B* **37,** 3759 (1988).
24. T. Ohta, F. Izumi, M. Onoda, M. Isobe, E. T. Muromachi, and A. W. Hewat, *J. Phys. Soc. Jpn.* **66,** 3107 (1997).
25. S. Shamoto, *Physica C* **341–348,** 1999 (2000).
26. A. Bianconi, G. Bianconi, S. Caprara, D. D. Castro, H. Oyanagi, and N. L. Saini, *J. Phys. Condens. Matter.* **12,** 10655 (2000).